Iraqi Journal of Physics, 2024 *Vol. 22, No. 1, PP. 10-19*

https://doi.org/10.30723/ijp.v22i1.1194

P-ISSN: 2070-4003
E-ISSN: 2664-5548

Spectral Analysis of Al Arc Discharge Plasma Generated in ZnO/DDDW Colloid

Mena L. Badran[1a*] and Saba. J. Kadhem[1b]
[1]*Department of Physics, College of Science, University of Baghdad, Baghdad, Iraq*
[b]E-mail: Saba.Kadhem@sc.uobaghdad.edu.iq
[a*]Corresponding author: mina.luay2204m@sc.uobaghdad.edu

Abstract

This study aims to investigate the aluminum (Al) arc plasma parameters generated through the explosive strip technique. The research involves the measurement of key plasma characteristics such as plasma frequency (f_p), Debye length, and Debye number. The electron temperature (T_e) and electron density (n_e) of the plasma were calculated utilizing the Boltzmann plot and Stark expansion method. Analysis of the optical emission spectrum revealed distinctive peaks corresponding to oxygen, Al, and zinc oxide (ZnO) within the plasma. The outcomes of the study demonstrated a noteworthy correlation between the applied current and the electron temperature and density. Specifically, as the current increases, both electron temperature and density increase. The electron temperature of the Al plasma increased from the range of 0.852 eV to 0.92404 eV, accompanied by a corresponding elevation in electron density from 13.1×10^{17} cm^{-3} to 15.2×10^{17} cm^{-3}. Furthermore, the detonation of the Al strip within a ZnO suspension led to even more pronounced changes. In this case, the electron temperature surged from 0.92885 eV to 1.1012 eV, and the electron density experienced an increase from 37.7×10^{17} cm^{-3} to 44.7×10^{17} cm^{-3}.

Article Info.

Keywords:
Al plasma, Al-ZnO Plasma, Electro-Exploding Wire, Plasma Diagnostic, Plasma Parameters.

Article history:
Received: Aug.26, 2023
Revised: Oct. 18, 2023
Accepted: Oct.31, 2023
Published: Mar. 01, 2024

1. Introduction

Electro explosion of wires (EEW) is a phenomenon that plasma physicists frequently exploit to generate plasma and synthesize nanoparticles [1, 2]. EEW is considered one of the promising techniques for producing nanoparticles and is considered one of the applications of electrical strip explosion. It is a simple, inexpensive and effective method to produce large quantities of high purity nanoparticles [3-6]. EEW has been used successfully in environmentally insensitive fast exploding wire detonators because it offers sufficient energy density for initiation of detonation required for the explosion. Such exploding wire detonators were used to cut bolts and control cables of rocket stages, as well as to initiate charges used to loosen frozen soil or rocks before housing construction. EEW was used in many other applications, too [7]. Forming nanoparticles inside a liquid is more efficient than in the air because of the speed of cooling of these particles, ensuring that these particles do not collect again, thus obtaining particles in the nanoscale range. EEW method in liquid has emerged as one of the most promising methods for producing metal nanoparticles [8, 9]. Underwater electrical wire explosions (UEWE) are accompanied by complex processes that include the creation of strong radiation fluxes, severe shock waves (SSW) in the aqueous medium, and phase changes of exploding wire metal-liquid-vapour plasma [10].

The aim of the research is to spectrally analyze the aluminum (Al) and Al /zinc oxide (ZnO) plasmas generated by the explosion wire technique and to study

the effect of the current supplied to the explosive system on the parameters of the generated plasmas.

2. Methodology

Many parameters, such as the supplied current, the diameter of the wires, and the nature of the surrounding environment, can influence the size and properties of the produced nanoparticles. Optical spectroscopy is an important method for diagnosing plasma. It is used to gather data about the nature of plasma, such as its species, density, temperature, and chemical composition [11]. In general, spectral diagnostic techniques seek to identify connections between plasma parameters and radiation characteristics, such as the strength of emission or absorption and the broadening or shifting of spectral lines.

The emission spectrum is frequently composed of several distinct atomic or ionic spectral lines [12]. The spectral line intensity (I_{ji}) is [13, 14]:

$$I_{ji} = \frac{N}{4\pi\lambda U(T)} g_j A_{ji} hc e^{\frac{-E_j}{k_B T_e}} \quad (1)$$

where: U(T) is the partition function, N represents the total number of levels, c is the velocity of light, g_j is the density of states, E_j denotes the energy of the upper level, A_{ji} denotes the transition probability between the upper level (j) and the lower level (i), and T_e is the electron temperature. The Boltzmann plot equation is one of the finest methods for determining the electron temperature in the local thermodynamic equilibrium [15]:

$$\ln\left(\frac{I_{ji}\lambda_{ji}}{hcg_j A_{ji}}\right) = \left(-\frac{E_j}{KT_e}\right) + \left(\frac{N(T)}{U(T)}\right) \quad (2)$$

where: λ_{ji} is the wavelength that corresponds to the transition between levels j and i.

The collisions in plasma cause Stark broadening of the spectral lines. A sharp broadening of an emission line or the linear density ratio of several emissions for the same element can be used to compute the electron density [16,17]. The electron density (n_e) can be calculated using the Stark broadening relation [18, 19]:

$$n_e(cm^{-3}) = \left[\frac{\Delta\lambda}{2\omega_s(\lambda, T_e)}\right] N_r \quad (3)$$

The reference electron density, denoted as N_r, is equal to 10^{16} cm^{-3} for neutral atoms and 10^{17} cm^{-3} for singly charged ions, ω_s represents the theoretical line derived with the same reference electron density, $\Delta\lambda$ is the full width at half maximum of the middle of the peak.

The process through which charged particles (ions and electrons) mitigate the effects of applied electric fields is known as Debye shielding. This shielding, a unique property of plasma, provides quasi-neutrality. The following equation can be used to calculate a distance (λ_D), also known as the Debye length [20]:

$$\lambda_D = \left(\frac{k_B T_e}{4\pi e^2 n_e}\right)^{\frac{1}{2}} \quad (4)$$

where: T_e and n_e are the electron temperature and density, respectively. The condition that must be met for plasma to exist is that the number of particles in the Debye sphere is greater than one ($N_D >>> 1$); this number is affected by electron density as well as electron temperature [21]:

$$N_D = \frac{4}{3}\pi \lambda_D{}^3 \quad (5)$$

The below formula is used to determine the plasma frequency [22]:

$$\omega_p = \sqrt{\frac{n_e e^2}{\epsilon_0 m_e}} \quad (6)$$

where: e is the electron charge, and ϵ_o is the permittivity of free space.

Plasma is formed when electrical strips explode when they touch the panel. Explosive strip technology can be controlled by several experimental parameters, including voltage, current pulse, material type, wire diameter, medium in which the explosion occurs, etc. [13]. The radiation emitted from this plasma must be examined to study the parameters of the plasma.

In this work, two plasmas were generated, the Al and the ZnO plasma. The effect of the current value supplied to the explosive system on the generated plasma parameters was investigated [23]. Also, spectroscopic analysis was carried out to study the Al and ZnO plasma generated by the explosion strip technique.

3. Experimental Part

Fig. 1 illustrates the set-up of the exploding wire system employed for the synthesis of metal nanoparticles in a liquid medium, conducted under atmospheric pressure, using the electrical explosion strip technique. The system comprises essential components, including a container with liquid media for the blasting process, a DC power supply rated at 250 V, wire guides, and a unit for wire supply. The first electrode, serving as the negative terminal, is a strip of Al 1 cm in width, 25 cm long and 0.1 cm thick. The second electrode, the positive terminal, is a (4.5 x 3.5) cm and 0.15 cm thick Al plate. It is noteworthy that the strip and the plate were made of the same metal, but with reverse polarity. Substantial electric currents (DC) ranging from 25 to 125 A were supplied through the Al components.

Upon contact between the negative electrode (the strip) and the positive electrode (the plate), the strip vaporises and transforms into plasma. Consequently, this process yields Al nanoparticles. High DC within the range of 25 to 125 A were applied to the Al strip in a liquid medium of double distilled deionized water (DDDW), and again the process was repeated in the presence of a suspension of ZnO in a liquid medium of DDDW, wherein 0.25 g of ZnO are introduced per 100 ml of DDDW. This procedure results in the production of ZnO nanoparticles adorned with Al.

The gathered data was accurately studied and compared with information sourced from the National Institute of Standards and Technology (NIST) database [24].

4. Results

4.1. Al Plasma

Fig. 2 presents the optical emission spectra (OES), obtained with UV-NIR spectrometer (Surwit, model S3000), of the plasma generated from the explosion of the aluminium strip, measuring 1 cm in width, 25 cm in length, and 0.1 cm in thickness at different values of supplied DC of (25, 50, 75, 100, and 125) A. The recorded spectra encompass a wavelength range of 320-1020 nm. All spectra obtained with the different electric currents showed multiple distinctive peaks corresponding to both Al atoms and ions, including (Al II at 466.30460nm, Al II at 624.30700nm, Al II at 704.20800nm, O II at 358.46610nm, O II at 383.30706nm, O I at 395.30000nm, O II at 434.20030nm, O II at 447.79060nm, O II at 485.67620nm, OII at 517.59030nm, OII at 558.3232nm, O II at 656.52830nm, O I at 777.53880nm and O I at 794.31500nm). Notably, the two highest peaks in the spectra are observed at 656.52830 nm, corresponding to oxygen

ions, and 395.30000 nm, indicative of oxygen atoms. Additionally, there are discernible peaks in the spectrum attributable to hydrogen and oxygen. The presence of hydrogen atoms can be attributed to the dissociation of water molecules.

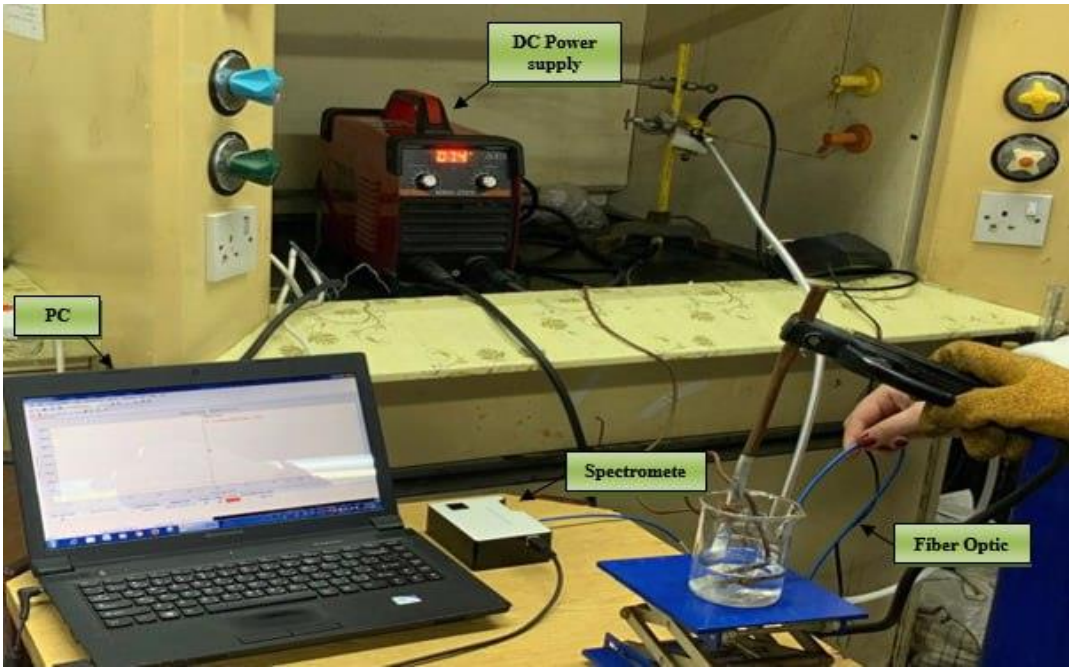

Figure 1: Exploding wire system.

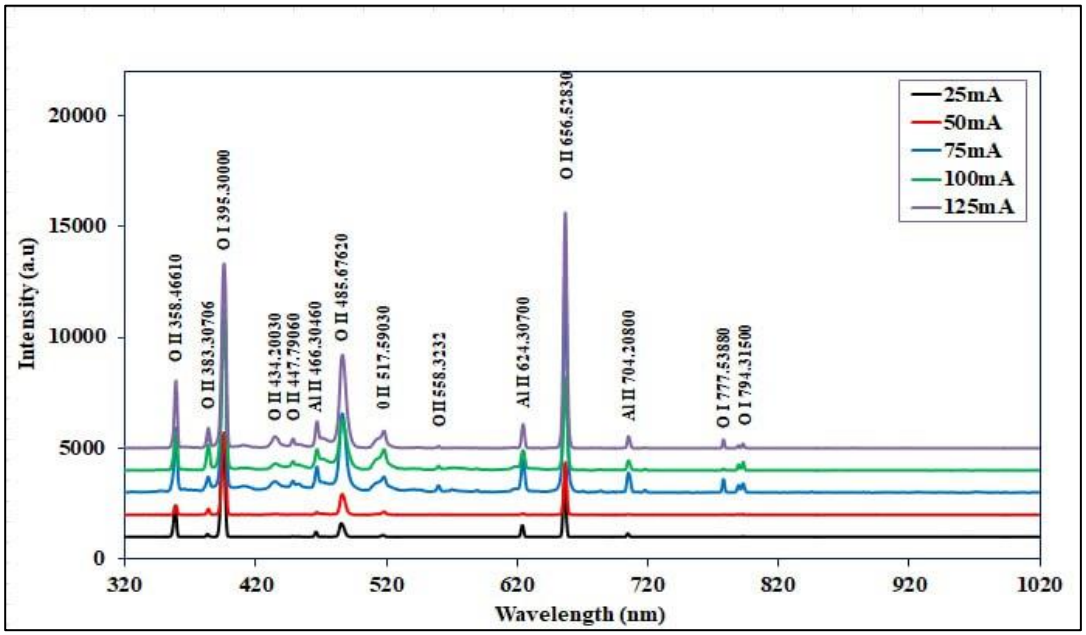

Figure 2: Emission spectra of aluminium plasma at different values of electrical DC current.

The electron temperatures (T_e) were determined by analyzing Boltzmann plots, which involve identifying peaks originating from the same atomic species and exhibiting the same ionization stage. To calculate T_e, five O II lines at wavelengths (358.4661, 383.30706, 485.6762, 517.5903 and 656.5283) nm for the different electrical current values of 25 to 125 A., were considered the parameters related to the upper energy levels, statistical weights, and transition probabilities employed for generating experimental plots for each element were sourced from the National Institute of

Standards and Technology (NIST) database. The electron temperature was derived from Boltzmann plots, the relationship between $ln(I_{ji}\lambda_{ji}/chg_jA_{ji})$ and the upper energy level (E_j) for the different values of current under investigation, as the reciprocal of the slope of the fitted line, as demonstrated in Fig. 3. The coefficient of determination (R^2), which ranges from 0 to 1, indicates the goodness of fit. The most favorable fits are those approaching a value of 1. The observed range of R^2 values in this study spans from 0.7032 to 0.7816.

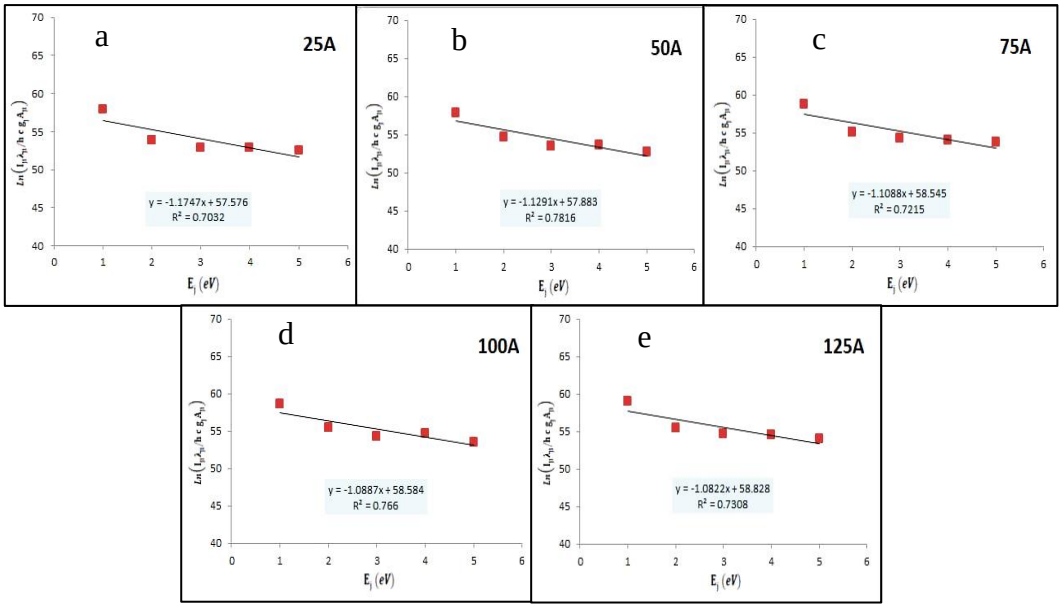

Figure 3: Boltzmann plots for O II lines generated by Al strip explosion at different values of electrical current.

Fig. 4 shows the changes of T_e and electron density (n_e) for Al with the different values of current.

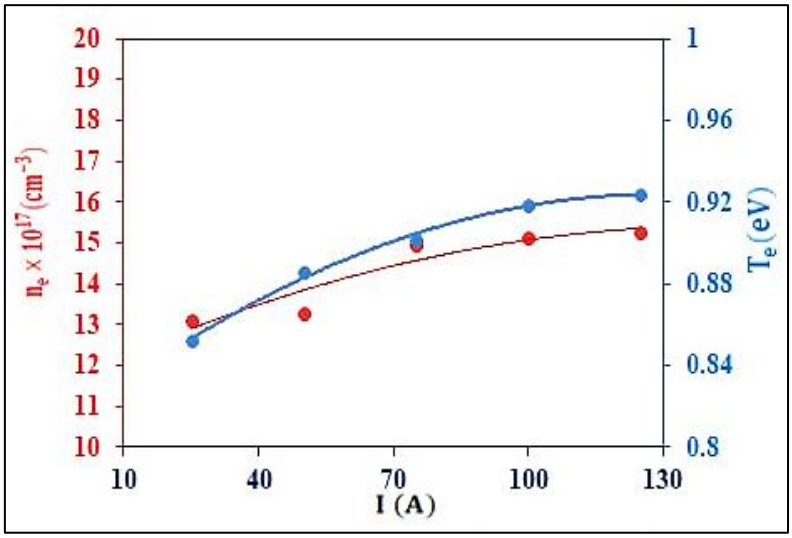

Figure 4: T_e and n_e of Al plasma change with the current.

T_e increases from 0.852 eV to 0.924 eV, while n_e rises from 13.1×10^{17} cm^{-3} to 15.2×10^{17} cm^{-3} as the current escalates from 25 A to 125 A. This result is consistent with the result of Sahai et al. [1].

Table 1: Coefficients of Al plasma for different values of current.

Current (A)	T_e (eV)	FWHM (nm)	$n_e \times 10^{17}$ (cm^{-3})	$\omega_p \times 10^{11}$ (rad/sec)	$\lambda_D \times 10^{-6}$ (cm)	N_d
25	0.852	2.56	13.1147541	647.2651571	0.598864453	1184
50	0.886	2.59	13.26844262	651.0466799	0.607149581	1248
75	0.9018	2.92	14.95901639	691.2794907	0.57691479	1207
100	0.9185	2.95	15.11270492	694.8215097	0.579247789	1235
125	0.9240	2.98	15.26639344	698.3455636	0.578050757	1239

Fig. 5 depicts the line profile of the Al plasma's 656.52 nm O II oxygen peak. Based on the numerical findings of the Lorentzian fitting line broadening, the whole width at half maximum was utilized to measure the electron density of plasma with varied currents using the Stark effect. The whole width grows as current increases, indicating an increase in electron density [15].

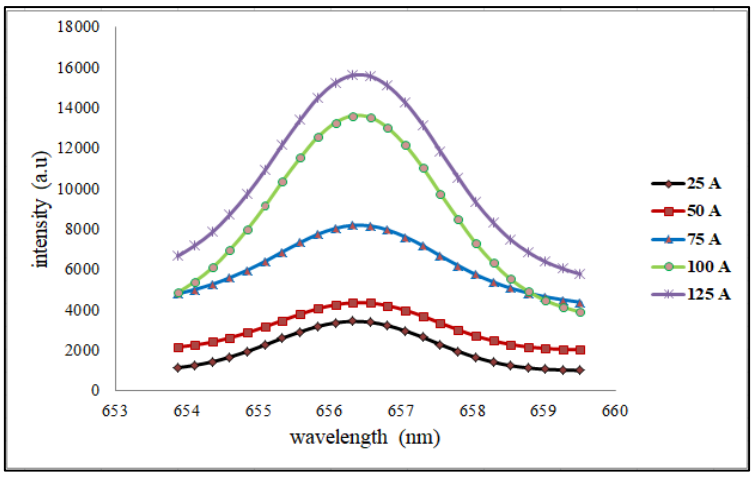

Figure 5: The O II oxygen peak expansion at 656.52 nm and Lorentzian fitting of Al plasma for the currents 25, 50, 75, 100 and 125A.

4.2. Al/ZnO Plasma

Fig. 6 displays the OES of plasma generated from Al strip under varying DC currents (25, 50, 75, 100, and 125) A in the presence of ZnO, encompassing a wavelength range of (320–1020) nm. The spectra showed numerous distinctive peaks corresponding to Al, atoms and ions, including (Al II at 434.7275nm, Al II at 466.3046nm, Al II at 515.823nm, Al II at 538.8682nm, Al II at 586.781nm, Al II at 660.964nm, Al II at 704.206nm, Al II at 781.231nm, Al III at 792.166nm, Zn I at 411.32100nm, Zn II at 492.40300nm, Zn I at 623.91690nm, O II at 383.6697nm, O I at 395.4607nm, O II at 448.4504nm and O II at 558.3232nm). Notably, the two highest peaks corresponding to Al ions are observed at 660.964 nm and for oxygen atoms at 395.4607 nm.

Additionally, discernible peaks in the spectrum are attributed to hydrogen and oxygen. The presence of hydrogen atom peaks results from the dissociation of water molecules.

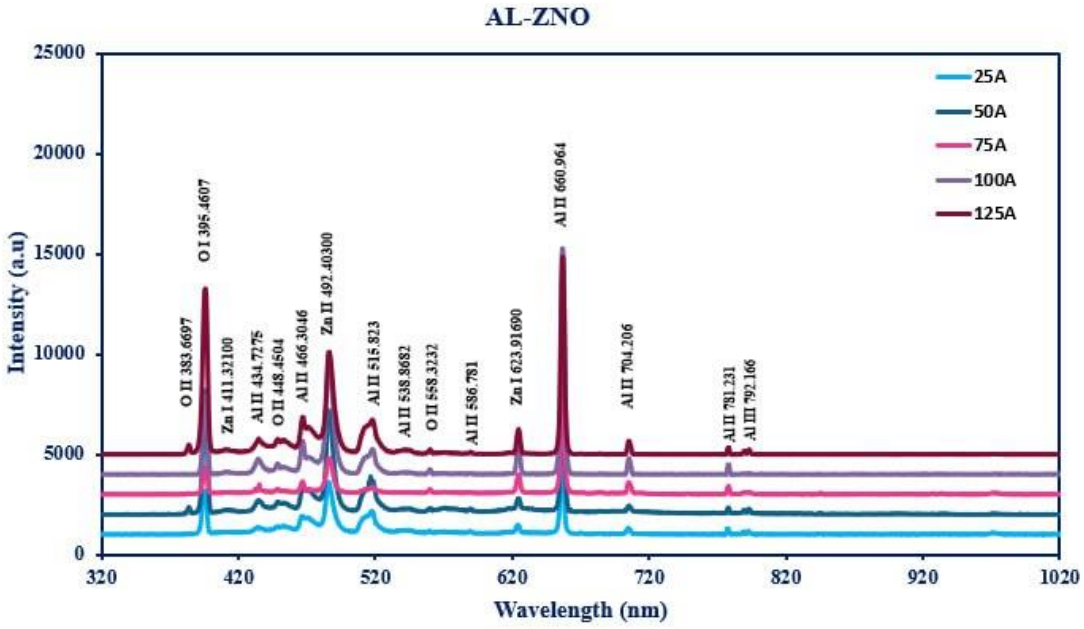

Figure 6: Emission spectra of Al plasma in the presence of ZnO at different currents.

The values of T_e were calculated by Boltzmann plots using five Al II lines at (515.823, 538.868, 434.727, 660.964 and 781.231) nm for different currents, as shown in Fig. 7. The T_e values were deduced from the reciprocal slope of the best fitting line of Boltzmann plots. Figs. 7(a-e) represent the relation between $ln\left(I_{ji}\lambda_{ji}/chg_jA_{ji}\right)$ and upper energy level (E_j) for the various current values. From the figures, it is noted that R^2 has a range of values from 0.854 to 0.897.

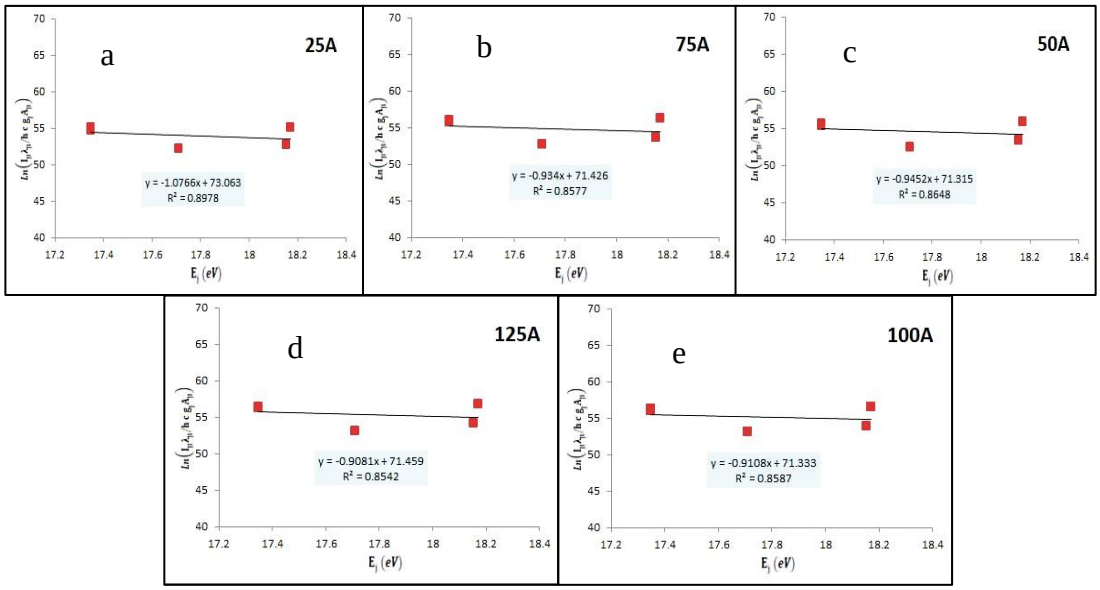

Figure 7: Boltzmann plots for Al and ZnO produced by EEW at various currents.

Fig. 8 shows the T_e and n_e changes of the Al strip with current of (25, 50, 75, 100, and 125) A in the presence of ZnO. Table 2 shows the Al/ZnO plasma parameters for various current values.

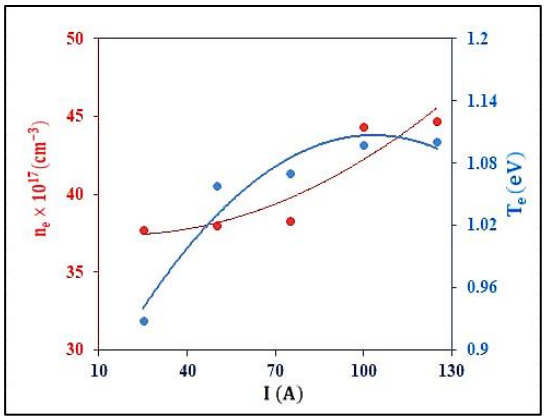

Figure 8: T_e and n_e of Al/ZnO plasma for currents of (25, 50, 75, 100, and 125) A.

Table 2: Al/ZnO plasma parameters for various current values.

Current (A)	T_e(eV)	FWHM(nm)	$n_e \times 10^{17}$ (cm^{-3})	$\omega_p \times 10^{11}$(rad/sec)	$\lambda_D \times 10^{-6}$(cm)	N_D
25	0.92885	2.87	37.76315789	1098.338748	0.368491483	794
50	1.05798	2.89	38.02631579	1102.159069	0.391909163	962
75	1.07066	2.91	38.28947368	1105.966192	0.392893555	976
100	1.09794	3.37	44.34210526	1190.173586	0.369717462	942
125	1.1012	3.4	44.73684211	1195.459357	0.368628792	942

As a result, a rise in the number of excited and ionized atoms during the ionization process implies an increase in electron density.

5. Discussions

The observed increase in the intensity of the Al plasma spectra, induced by the explosive wire method, with the increase of the current of the explosion circuit, can be ascribed to a confluence of interdependent factors that impact the behavior of the plasma, as demonstrated in Figs. 2 and 5, these factors are:

1. Electron density: Increasing the current in the explosion circuit results in more electrons being released into the plasma. This higher electron density leads to enhanced collision frequency and increased excitation of atoms and ions in the plasma, subsequently leading to more intense emission of radiation [25].
2. Enhanced ionization: increasing the current leads to more ionization of the Al atoms in the explosive plasma. Thus, more electrons are stripped from the Al atoms, resulting in a larger number of highly excited ions. As these ions relax to lower energy states, they emit photons with characteristic frequencies, contributing to the intensity of the plasma spectra.
3. Electron temperature: The higher current can also increase the electron temperature of the plasma. Higher electron temperatures mean that electrons possess higher kinetic energies, which allows them to access higher energy states and promote stronger emission of radiation as they transit to lower energy states [26].
4. Energy input: The increase in current translates to a greater energy input into the plasma. This added energy accelerates the motion of charged particles, leading to more frequent collisions and higher energy-level excitations. These collisions

provide the necessary energy to excite atoms and ions to higher energy levels, causing them to emit radiation as they return to their ground states.

All of the spectra shown in Figs. 2 and 5 demonstrate that as the current density grew, the intensity of the peaks increased. As the current increases, the power supplied to the electrical circuit increases. Consequently, the energy given to the atoms increases, resulting in higher temperature and density of the plasma.

It is evident from Figs. 4 and 7, as well as Tables 1 and 2, for the Al and Al/ZnO plasma spectra that as the current of the explosion circuit increases, so does the electrons temperature and density in the Al and Al/ZnO plasmas produced by the explosive wire method. The higher detonation current results in an increased amount of energy being deposited into the plasma. This additional energy accelerates electrons, ions, and atoms in the plasma, leading to more frequent collisions. These collisions contribute to the heating of electrons, raising their kinetic energies and, consequently, their temperature [27].

Also, increasing the current causes more Al atoms to lose electrons and become ions. This increased ionization leads to a higher density of free electrons, as well as a higher density of ions. More free electrons are available to participate in collisions, leading to more efficient energy transfer and electron heating [28].

Tables 1 and 2 present data that indicates an increase in the plasma frequency when the current was increased. The plasma frequency is proportional to the square root of the electron density, which increases as the current increases. So, when the current increases the plasma frequency increases also. Regarding the Debye length, it can be observed that while there is some fluctuation in its value, in general, increasing the electron density leads to a decrease in the Debye length. This is due to the fact that a higher electron density results in stronger screening of electric fields, causing the plasma to behave like a neutral medium over shorter distances. When the current is increased, there are more electrons within the Debye sphere, which raises the Debye number, reflecting the larger number of charged particles within the defined scan region determined by the Debye length.

6. Conclusions

In this study, a thorough investigation of Al arc plasma parameters generated via the explosive wire technique was undertaken. Valuable insights into plasma behavior were achieved by carefully examining key parameters like electron temperature (T_e), electron density (n_e), and plasma frequency (ω_p). The electron temperature and density of the plasma were accurately calculated employing Boltzmann plots and the Stark expansion method. The results revealed a substantial correlation between the applied supply current and both the electron temperature and density. The spectroscopic analysis was very important for giving us important details about the Al and ZnO plasma that was made using the explosive wire technique. The results showed that increasing the applied explosive current led to higher emission intensity, T_e, n_e, full width at half maximum (FWHM), and ω_p, which was attributed to the higher power supplied to the system.

Conflict of Interest

Authors declare that they have no conflict of interest.

References

1. A. Sahai, N. Goswami, S. Kaushik, and S. Tripathi, Appl. Surf. Sci. **390**, 974 (2016).

2. Y. Hu, H. Shi, T. Li, Z. Tao, X. Li, J. Wu, Y. Zhang, and A. Qiu, IEEE Trans. Plasma Sci. **50**, 2520 (2022).
3. R. Sarathi, T. Sindhu, and S. Chakravarthy, Mat. Charact. **58**, 148 (2007).
4. S. H. Abdullah, H. R. Humud, and F. I. Mustafa, Iraqi J. Sci. **63**, 4273 (2022).
5. P. Sen, J. Ghosh, A. Abdullah, P. Kumar, and Vandana, J. Chem. Sci. **115**, 499 (2003).
6. R. K. Tekade, *Biomaterials and Bionanotechnology* (London, UK, Academic Press, 2019).
7. Y. A. Kotov, J. Nanopar. Res. **5**, 539 (2003).
8. A. S. Wasfi, H. R. Humud, and N. K. Fadhil, Opt. Laser Tech. **111**, 720 (2019).
9. A. Alqudami and S. Annapoorni, Plasmonics **2**, 5 (2007).
10. S. Wagner, A. Gondikas, E. Neubauer, T. Hofmann, and F. Von Der Kammer, Angewandte Chem. Int. Ed. **53**, 12398 (2014).
11. T. Namihira, S. Sakai, T. Yamaguchi, K. Yamamoto, C. Yamada, T. Kiyan, T. Sakugawa, S. Katsuki, and H. Akiyama, IEEE Trans. Plasma Sci. **35**, 614 (2007).
12. K. A. Aadim and A. A. Yousef, Iraqi J. Sci. **59**, 494 (2018).
13. H. R. Humud, Iraqi J. Phys. **15**, 142 (2017).
14. K. A. Aadim, Iraqi J. Phys. **15**, 65 (2017).
15. M. M. Shehab and K. A. Aadim, Iraqi J. Sci. **62**, 2948 (2021).
16. A. K. Bard and Q. A. Abbas, Optik **272**, 170346 (2023).
17. M. J. Ketan and K. A. Aadim, Iraqi J. Sci. **64**, 188 (2023).
18. N. Shaikh, S. Hafeez, B. Rashid, and M. Baig, Euro. Phys. J. D **44**, 371 (2007).
19. W. Kim, J.-S. Park, C.-Y. Suh, S.-W. Cho, and S. Lee, Mat. Trans. **50**, 2344 (2009).
20. H. I. Hussein and K. A. Aadim, Iraqi J. Sci. **63**, 971 (2022).
21. M. M. Kadhim, T. H. Khalaf, and Q. A. Abbas, Iraqi J. Sci. **63**, 4771 (2022).
22. H. Q. Farag and S. J. Kadhem, Iraqi J. Phys. **20**, 45 (2022).
23. N. K. Hussein and S. Kadhem, Iraqi J. Sci. **63**, 2492 (2022).
24. Y. Ralchenko and A. Kramida, Atoms **8**, 56 (2020).
25. H. Hashim, Al-Nahrain J. Sci. **21**, 88 (2018).
26. M. A. Mohammed, H. N. Hashim, and K. A. Aadim, J. Opt., 1 (2023).
27. N. Konjević, A. Lesage, J. R. Fuhr, and W. L. Wiese, J. Phys. Chem. Ref. Data **31**, 819 (2002).

تحليل طيفي للتفريغ القوسي لبلازما الألمنيوم المتولدة داخل عالق من ZnO/DDDW

مينا لؤي بدران[1] وصبا جواد كاظم[1]

[1]قسم الفيزياء، كلية العلوم، جامعة بغداد، بغداد، العراق

الخلاصة

تهدف هذه الدراسة إلى حساب متغيرات قوس بلازما الألمنيوم المتولدة بتقنية الشريط المتفجر. يتضمن البحث قياس خصائص البلازما الرئيسية مثل تردد البلازما (f_p)، وطول ديباي، وعدد ديباي. تم حساب درجة حرارة الإلكترون (T_e) وكثافة الإلكترون (n_e) للبلازما باستخدام مخطط بولتزمان وطريقة توسع ستارك. كشف تحليل طيف الانبعاث البصري عن قمم مميزة تتوافق مع الأكسجين والألومنيوم وأكسيد الزنك داخل البلازما. أظهرت نتائج الدراسة وجود علاقة ملحوظة بين التيار المطبق ودرجة حرارة الإلكترون وكذلك الكثافة. على وجه التحديد، مع زيادة التيار، أظهرت كل من درجة حرارة الإلكترون وكثافته ارتفاعًا متناسبًا. زادت درجة حرارة الإلكترون في بلازما الألومنيوم من نطاق 0.852 فولت إلى 0.92404 فولت، مصحوبة بارتفاع مماثل في كثافة الإلكترون من 131,1 × 10^{17}سم$^{-3}$ إلى 152,6 ×^{17} 10 سم $^{-3}$. علاوة على ذلك، أدى انفجار شريط الألمنيوم داخل معلق أكسيد الزنك إلى تغييرات أكثر وضوحًا. في هذه الحالة، ارتفعت درجة حرارة الإلكترون من 0.92885 فولت إلى 1.1012 فولت، وشهدت كثافة الإلكترون زيادة من 377,6 ×10^{17} سم$^{-3}$ إلى 447,4 × 10^{17} سم$^{-3}$.

الكلمات المفتاحية: بلازما الالمنيوم، بلازما أكسيد الزنك، الأسلاك الكهربائية المتفجرة، تشخيص البلازما، معلمات البلازما.